Nanoscale

Accepted Manuscript

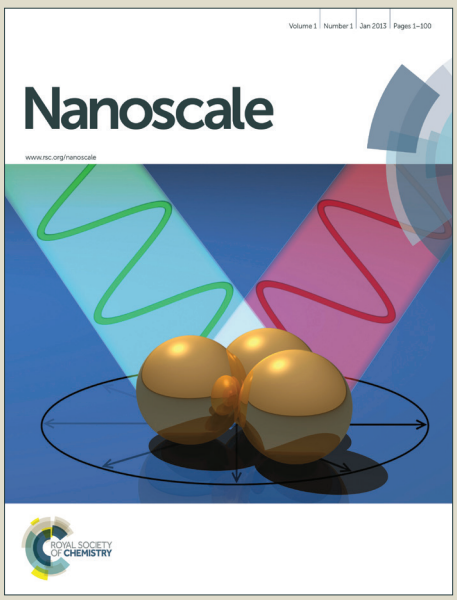

ROYAL SOCIETY OF CHEMISTRY

www.rsc.org/nanoscale

Single-cell correlative nanoelectromechanosensing approach to detect cancerous transformation: Monitoring the function of F-actin microfilaments in the modulation of ion channel activity

Mohammad Abdolahad[1,2*#], Ali Saeidi[1,2#] , Mohsen Janmaleki[3#], Omid Mashinchian[4†], ,Mohammad Taghinejad[7†], Hossein Taghinejad[7†], Soheil Azimi[1,2] †, Morteza Mahmoudi[5,6*†], Shams Mohajerzadeh[1,2*#]

[1]Nanoelectronic Center of Excellence, Thin Film and Nanoelectronic Lab, School of Electrical and Computer Engineering, University of Tehran, P.O. Box 14395/515, Tehran, Iran

[2]Nano Bio Electronic Devices Lab, School of Electrical and Computer Engineering, University of Tehran, P.O. Box 14395/515, Tehran, Iran

[3]Medical Nanotechnology and Tissue Engineering Research Center, Shahid Beheshti University of Medical Sciences P.O. Box 1985717443 Tehran, Iran

[4]Department of Medical Nanotechnology, School of Advanced Technologies in Medicine (SATiM), Tehran University of Medical Sciences, P.O. Box 14177-55469, Tehran, Iran

[5]Department of Nanotechnology & Nanotechnology Research Center, Faculty of Pharmacy, Tehran University of Medical Sciences, P.O. Box 14155-6451, Tehran, Iran

[6] Division of Pediatric Cardiology, Department of Pediatrics, Stanford University School of Medicine, Stanford, California 94305-5101, USA

[7] Nanophotonic Research Group, School of Electrical and Computer Engineering, Georgia Institue of Technology 777 Atlantic Drive NW Atlanta Georgia 30332 USA

* Corresponding Authors: m.abdolahad@ut.ac.ir, mohajer@ut.ac.ir, mahmoudi@stanford.edu

#, † : Authors with same contributions

Abstract

Cancerous transformation may be dependent on correlations between electrical disruptions in the cell membrane and mechanical disruptions of cytoskeleton structures. Silicon nanotube (SiNT)-

based electrical probes, as ultra-accurate signal recorders with subcellular resolution, may create many opportunities for fundamental biological research and biomedical applications. Here, we used this technology to electrically monitor cellular mechanosensing. The SiNT probe was combined with an electrically activated glass micropipette aspiration system to achieve a new cancer diagnostic technique that is based on real-time correlations between mechanical and electrical behaviours of single cells. Our studies demonstrated marked changes in the electrical response following increases in the mechanical aspiration force in healthy cells. In contrast, such responses were extremely weak for malignant cells. Confocal microscopy results showed the impact of actin microfilament remodelling on the reduction of the electrical response for aspirated cancer cells due to the significant role of actin in modulating ion channel activity in the cell membrane.

1. Introduction

Cancer is recognised as a type of disease that affects many biochemical,[1,2] electrical,[3,4] and mechanical functions of a cell.[5] Cytoskeletal alterations,[6,7] damping of electrodynamic microtubule oscillations,[8,9] diminution of dielectric properties of the membrane, and disruption in ion channel activity[10] are some of the considerable mechanical and electrical alterations in cells during cancerous transformation. For instance, the membrane composition of cancer cells becomes altered, and higher permeability of the membrane results in the movement of K^+, Mg^{++}, and Ca^{++} out of the cell and the accumulation of Na^+ and water inside the cell. Therefore, current across the membrane of cancerous cells is increased.[3] Highly accurate methods for monitoring such alterations in single cells could detect cancerous transformation in its early stages. Many reports have been published on the electrical,[11,12] mechanical,[13] and electro-optical[14] monitoring of single cells. In the case of electrical recording, high spatial resolution contacts between electrical probes and single cells are critical for both fundamental biophysical studies and disease monitoring.[15] The size of these probes was a challenge for noninvasive recording (particularly for the bioelectrical signals, which are weaker than action potentials) with subcellular-level resolution.[16-20]

Nanoscale electrical probes (e.g., conductive silicon nanowires and silicon nanotubes (SiNT))[21] have opened new fields of investigation, leading to the emergence of exciting future applications in cell bioelectrical and electrophysiological studies.[22-25] Recently published nanoprobe-based intracellular electrical recording methods have been applied solely for action potential measurements of some special types of electrically active cells with sharp responses, such as neurons and cardiomyocytes.[11,25] Such devices have been used to monitor the electrical activities of cells based on measuring the potential change outside the cell associated with the

transmembrane change of the cell in its excited state.[11,26,27] Although an action potential recording contains important details needed to understand the properties of ion channels during depolarisation and hyperpolarisation, the large amplitude of action potential signals and the restricted applications to neuronal cells make this type of recording an ineffective approach for detecting the minor electrical variations in epithelial cells caused by external or internal disruptions. The electrical behaviour of epithelial cells during disease progression, e.g., cancerous transformation, is such that the opening/closing of the ion channels as well as dielectric disruptions in membrane phospholipids define minor specific features/phases of membrane electrical signals. Therefore, their electrical responses are considerably weaker compared to neuronal cells. Despite the observable improvements in new generations of electrical nanoprobes,[11,28] no report has been published on the application of SiNT-based single-cell intracellular recording to monitor the bioelectrical disruption in cells such as cancerous progression. Furthermore, the correlation between the mechanical and electrical behaviour of a single cell, especially for use in cancer diagnosis, is unexplored.

Here, we combined the mechanical stimulation of a cell with intracellular electrical recordings using SiNT probes, which were grown on tungsten needles, to detect the cancer cells using a new nanobioelectromechanical concept. The effect of mechanical aspiration on normal and malignant cells stretched by an electrically activated glass micropipette was monitored for the bioelectrical response of the cell. This new approach for cancer diagnosis was named "correlative nanoelectromechanosensing of single cells for cancer diagnosis." This method thoroughly documents distinct changes in the electrical properties of the cell between normal and malignant states during the mechanical aspiration. Our results suggest that healthy cells have a pronounced increase in the electrical response (impedance and phase) to the mechanical aspiration, whereas

the response is reduced for cancerous cells. Such a response may occur due to the critical role of actin microfilaments in the modulation of ion channel activity, as shown using confocal microscopy. This procedure should be considered as a new label-free nanoelectromechanical cancer diagnosis model with single-cell resolution.

2. Methods and Materials

2.1 SiNT/ W nanoprobe manufacture

A tungsten (W) needle as the supporter of SiNT nanoprobe was manufactured using an electrochemical etching process. SiNT was grown on the tip of the W needle (Fig. S1 A and B and S2). The growth process began by cleaning the needle with a solution of acetone and Buffer HF. Subsequently, the cleaned needle was held in an electron beam coating system (Veeco Co.) to deposit the Ni/Au catalyst bilayers. The needle was placed in a position in which the top of the needle was located in front of the target plume. The deposition was begun at a base pressure of 10^{-6} Torr. A thin layer of gold, with a thickness ranging from 1 to 4 nm was coated on top of the probe. Subsequently, another layer of nickel (10−40 nm) was coated over the gold layer. The growth of SiNT was achieved in a low pressure chemical vapour deposition (LPCVD) chamber (SensIran Co.) at a base pressure of 1 mTorr and at temperatures ranging from 400 to 600°C. Field emission electron microscopy (FE-SEM) and transmission electron microscopy (TEM) from the tube is shown in Figure 1B-4.

To enhance the electrical conductivity of nanotubes, they were held in phosphorous doping furnace in a temperature of 700 ^{o}C for 10 min. Furthermore, 5nm gold layer was coated on top of the tubes by the assistance of sputtering system. On the other hand, the nozzle of glass micropipette was coated by gold layer (10 nm) in the sputtering system. Then, both W/SiNT

probe and glass micropipette were installed on microinjection microscope and connected to readout system, by coaxial wires, to reduce the electrical noise (Figure S6).

2.2 Characterization of Actin Filament Deformation by Confocal Microscopy

The effects of cancerous transformation and cell aspiration on actin microfilament distribution, on stretched and control MRC-5 and QU-DB cell samples were assessed by inverted Confocal microscopy (Leica, TCS SP5, Germany). Prior to imaging, cells were fixed in 4% formaldehyde for 15 min and permeabilized with Triton X-100 in PBS (with the concentration of 1%) for 5-10 min at room temperature. Then, all samples were washed and stained with phalloidin-FITC conjugate (Green) (Sigma-Aldrich) and incubated for 30-45 min. The cell nuclei were stained with propidium iodide (PI) (Invitrogen, USA). The Leica Application Suite Advanced Fluorescence (LAS AF) software (Leica Microsystems) was utilized to analyze the confocal microscope pictures.

2.3 Cell aspiration process

A movable water reservoir was implemented to apply negative and positive pressure at the end of the glass micropipette. Displacing the reservoir up or down leads to suitable pressure to pull in or force away cell respectively. This is also applicable to find zero pressure. Meanwhile a precise digital ruler was showing the displacement which was related to actual pressure directly. The step constant negative pressure imposed to each cell maintained to be between 50-60 Pa in all experiments.

Aspirated leading edge of the cell surface was monitored by an inverted microscope (Nikon Eclipse) equipped with a digital camera (Nikon DXM1200). Internal diameters of micropipettes

were within range of 4.5μm to 5μm. A micromanipulator (Transfer Man Nk2, Eppendorf) was utilized to adjust each micropipette position. Analysis of images was performed by Axiovision LE Software (Zeiss).

3. Results and discussion

3.1 Structure and mechanism of the sensing system.

Our target for the electromechanical investigation of single cells (incorporating a SiNT/ tungsten (SiNT/W) electrical probe (Figure 1 A,B) and a gold-coated glass micropipette) has several key features to record critical data regarding the diagnostic effect of mechanical stimulation on the bioelectrical response differences between normal and malignant cells.

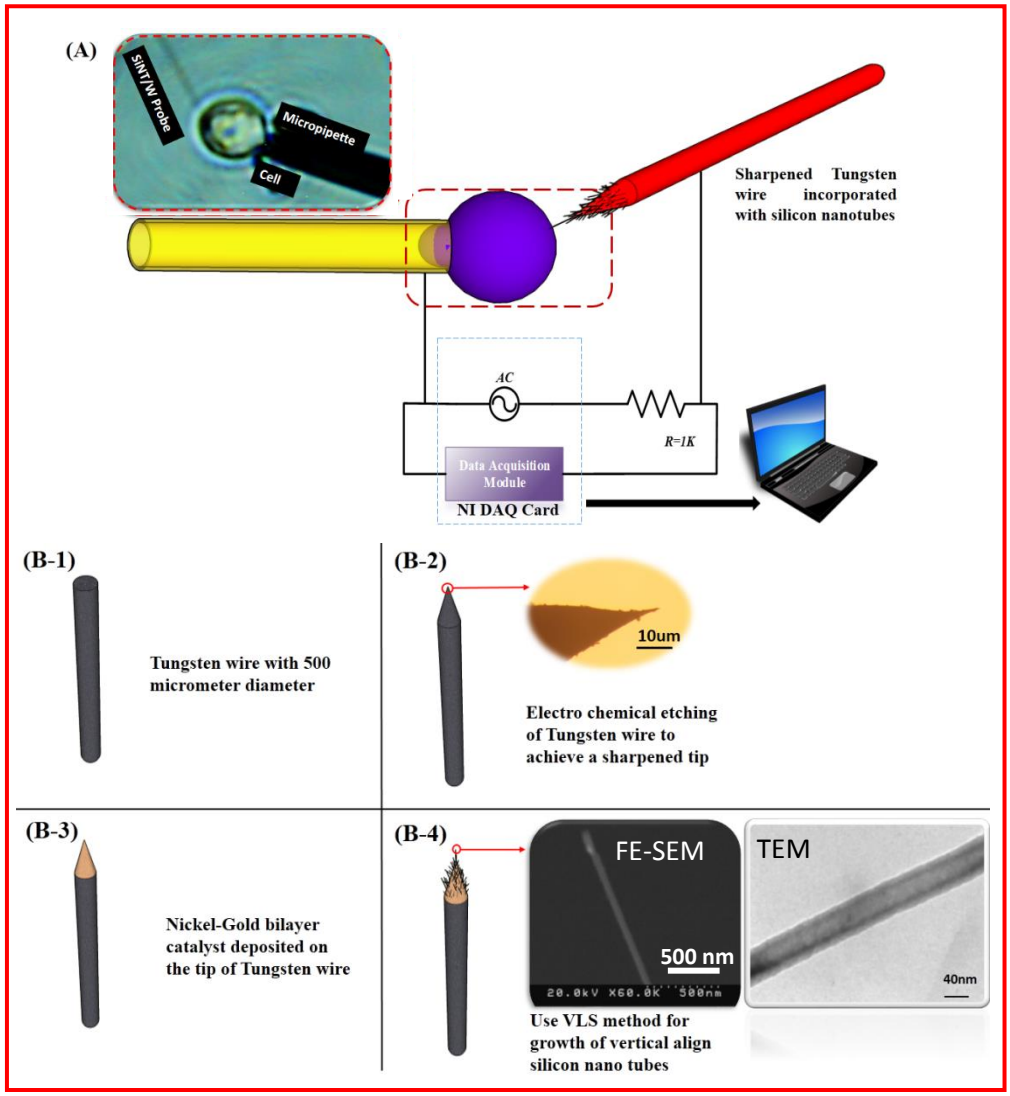

Figure 1. Schematic of a single-cell correlative nanoelectromechanosensing system and the nanoprobe manufacturing process. A) Schematic showing the features of the combined W/SiNT-micropipette system. The real-time electrical response was recorded for normal and cancerous single cells aspirated with similar suction forces. Top left: The optical images of the experimental cell. The trace of SiNT is observable due to optical diffraction. B) Manufacturing process of the SiNT/W nanoneedle. The tungsten tip was sharpened by electrochemical etching (1-2); the optical image of the formed W needle is shown in B-2. The Ni/Au bilayer catalyst was coated on the tip of the tungsten needle (3). Lastly, aligned SiNT was grown on top of the W needle using the VLS method. SEM and TEM images of the SiNT probe are shown in B-4.

This will create a new tool for cancer diagnosis based on the bioelectromechanical monitoring of the cell to enable sufficient electrical sensitivity derived from the mechanical stimulation. First, the doped SiNT probe, supported by the W needle, has a long free-end with thin walls for superficial and negligibly invasive cell penetration, which ensures high electrical sensitivity of the probe. Second, a pyramidal-shaped W needle (with ~ 100 nm cone radius shown in Figure 1-B-2) with significant electrical conductivity is used for the bottom element of the Si nanotube to provide mechanical stability during penetration. Third, a conventional glass micropipette used as an instrument for single-cell aspiration was coated with gold on the nozzle to function as the ground potential relative to the cell. This instrument provides a real-time electrical measurement from a single cell during mechanical aspiration in which a closed electrical circuit is applied between the SiNT and the micropipette (Figure 1-A).

To enhance the structure of the device, we developed an efficient, noncomplex and inexpensive multistep synthesis and manufacturing approach (Fig. 1-B), which is described in the Methods

section. First, the W nanoneedle was fabricated using an electrochemical etching process (Figure S1 and S1 text of Supporting Information (SI)). Next, the SiNT electrical nanoprobe was fabricated on the tip of the W needle (as a substrate surface). Briefly, a Ni/Au multilayer catalyst was grown on top of the W probe by low-pressure chemical vapour deposition (LPCVD) using our previously established method[29] (Figure 1 B-3,4). The electrical conductivity of the SiNT structure was noticeably enhanced by both phosphorous doping and Au coating (~ 5 nm) on the tip of the nanotubes as determined by a lifetime measurement (Figure S2 and S2 text of SI). Both the SiNT nanoprobe and the electrically activated glass micropipette were assembled on a microinjection microscope system (NARISHIGE Co. Japan) and connected to a readout system (NI DAQ USB 6323) (Figure S3 of SI). The basic electrical sensitivity of the device was characterised by placing the sensing system in an ionic solution (Figures S4-A and C, S3 text of SI), followed by comparing the sensitivity after connecting the system to the cell (Figure S4-B and C), and finally by scaling with dry ambient (Figure S4-C and E). The magnitude of the impedance (device sensitivity) decreased when the ambient was changed from air to a cellular media solution with a fixed distance between the SiNT and the micropipette (~ 7 μm).

3.2 Nanoelectromechanosensing of a single lung cell.

To investigate the electromechanical behaviour of a single cell, we characterised the electrical response (impedance magnitude and phase) of normal and malignant single cells aspirated by similar suction forces. The nozzle inner diameter of the glass micropipette was 5 μm. Healthy lung (MRC-5) and cancer (QU-DB) cells as well as colon primary (HT-29) and progressive (SW-48) malignant cells were cultured for this study. The culture process is discussed in the Supporting Information (S4 text of SI).

Figures 2A-D show the results of the SiNT probe-based electrical measurements from aspirated MRC-5 (Fig 2-A and B) and QU-DB (Fig 2-C and D) cells with various suction forces. Such forces resulted in different lengths of the cell that flowed into the pipette (L_p) due to the mechanical properties of each individual cell. Because the L_p value was determined from microscopic images (Fig 2-I and J), Young's modulus (E) as well as the applied pressure on the aspirated cell (ΔP) were measured using a micropipette aspiration method as discussed in the Supporting Information (Figure S5-6 and S5 text of SI). Table 1 shows the E, Lp, and ΔP of each cell that was aspirated by various suction forces (F_1, F_2 and F_3).

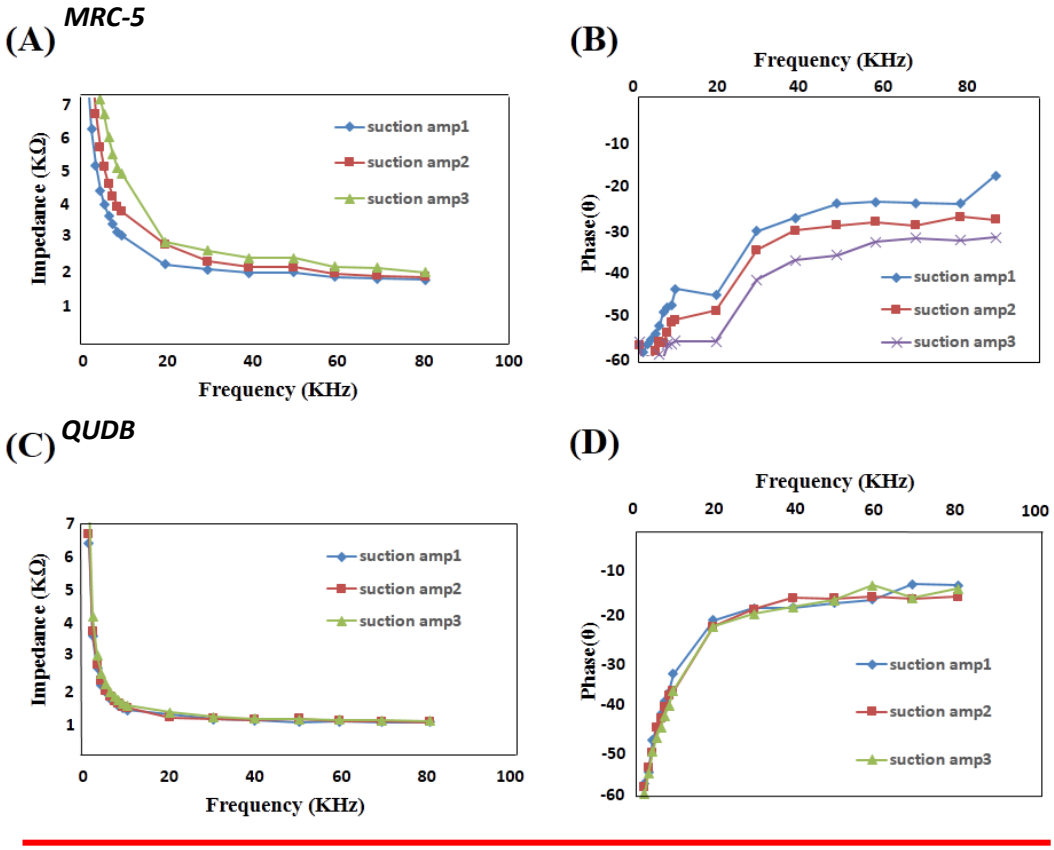

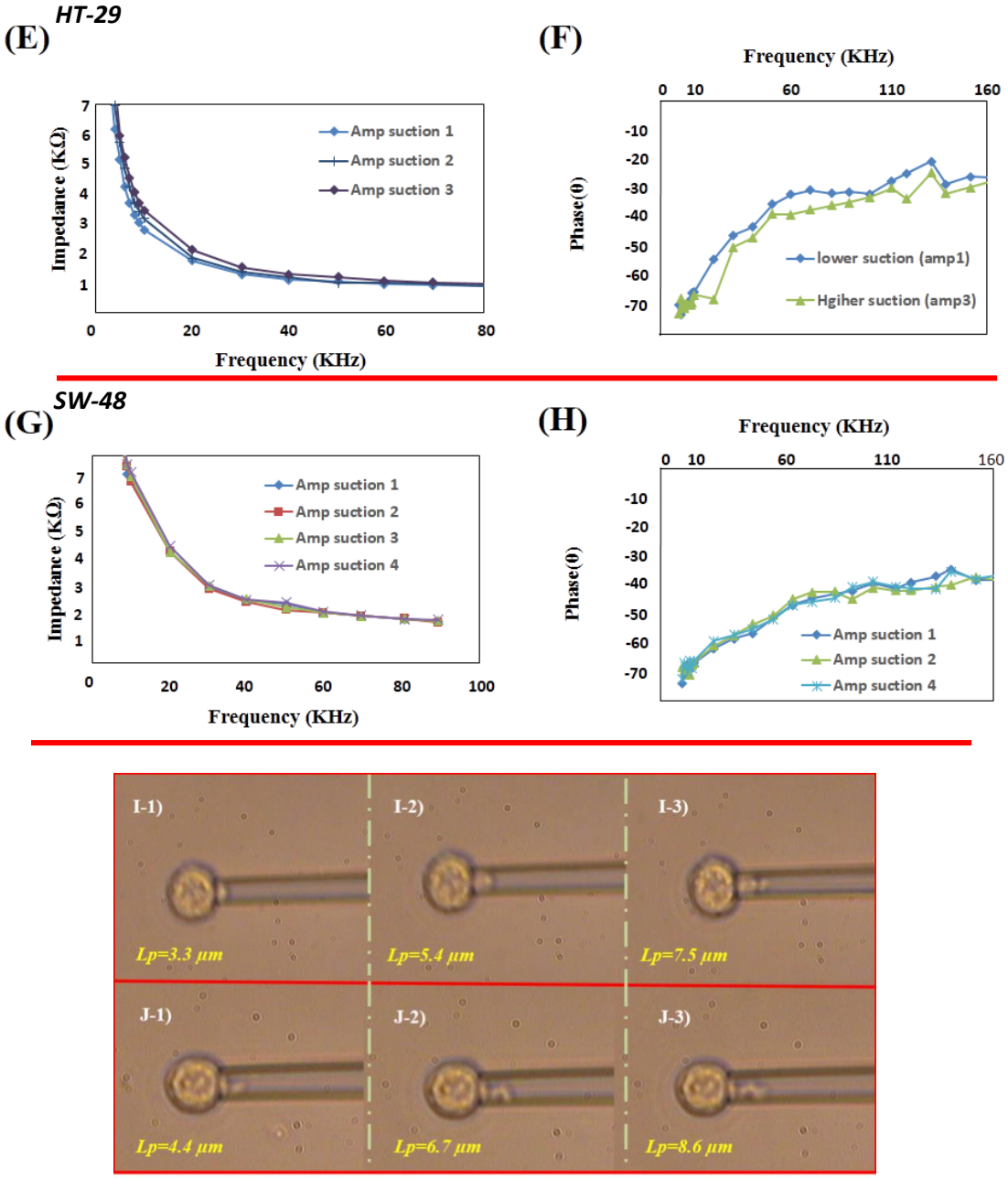

Figure 2. Mechanical aspiration induced significantly higher variations in the electrical response of normal cells compared to malignant cells. A) Impedance and B) phase responses of an aspirated MRC-5 single cell with three different suction amplitudes ranging from F_1 to F_3. The same experiment with similar suction forces was performed using QUDB, HT-29 and SW-48 single cells as shown in the diagrams of C-D, E-F and G-H. Changes in the electrical responses due to mechanical aspiration are more observable for healthy (MRC-5) and benign (HT-29) cells than for cancerous (QU-DB) and metastatic

(SW-48) cells. For better observation of the curves the error bars weren't plotted in the figure and just the standard deviations (Std. Dev) were indicated. Optical microscopy images of HT-29 (I_1-I_3) and SW-48 (J_1-J_3) single cells aspirated using a micropipette with different suction forces ranging from F_1 to F_3. The length of the cell flowed into the pipette (L_p), which is dependent on the cell's deformability (a key parameter in our measurements), is shown in the image.

Table 1. Mechanical parameters (E, Lp and ΔP) of aspirated cells using various suction forces ranging from F_1 to F_3.

Cell type	E (pa)	F_1		F_2		F_3	
		L_p (µm)	ΔP (pa)	L_p (µm)	ΔP (pa)	L_p (µm)	ΔP (pa)
QU-DB	92	4	674.09	6	970.63	8	1294.18
MRC-5	213	2.5	936.34	4.5	1685.42	5.8	2172.32
SW-48	84.6	4.4	654.54	6.7	1067.7	8.6	1309.09
HT-29	123.47	3.3	716.46	5.4	1172.39	7.5	1628.32

The representative recorded data, following a predictive model, show a clear increase in the cell impedance with increasing mechanical stretch amplitudes in healthy cells, whereas no noticeable impedance changes were observed in malignant cells after increasing the aspiration with the same suction forces. Changes in the bioelectrical parameters initiated from mechanical aspiration in healthy lung cells (MRC-5) were 10 times higher than those of aspirated cancerous cells (QU-DB) (Table 2). These results suggest that the bioelectrical properties of a healthy cell have a strong correlation with its mechanical function.

3.3 Detection of cell metastasis progression.

To further elucidate the effect of metastasis progression of cancer cells on their decrease in electromechanical response, we performed experiments on colon primary (HT-29) and progressive (SW-48) malignant cells. The obtained results (see Figure2 E-H) confirmed our proposed hypothesis. The average impedance and phase variation of an aspirated HT-29 cell were approximately 2-fold higher than those of a SW48 cell (Table 2).

Table 2. Change in cell electrical parameters due to mechanical aspiration.

Cell type	L_P (μm)	ΔImp_{ave} (Ω)	$\Delta Phase_{ave}$ (°)
QU_DB	4 →	190.5	0.73
	6 →	88.2	0.52
	8		
MRC-5	2.5 →	2776.76	4.01
	4.5 →	2382.1	3.74
	5.8		
SW-48	4.4 →	133.4	0.71
	6.7 →	74.8	0.21
	8.6		
HT-29	3.3 →	272.1	1.46
	5.4 →	222.6	1.17
	7.5		

Confocal microscopy images from non-aspirated (Figure3A) and aspirated (Figure 3B) QU-DB, and MRC-5 (Figure 3C and D, respectively) cells clearly show the effect of mechanical aspiration on changes in the distribution and architecture of actin filaments (detailed procedures for confocal microscopy are discussed in the Methods section). Although the mechanical

aspiration alters the actin microfilament configuration of both normal and malignant cells, the impedance of the cancer cells showed no alteration following the aspiration process. This may indicate strong differences in the correlation of bioelectrical/mechanical behaviours between normal and cancer cells.

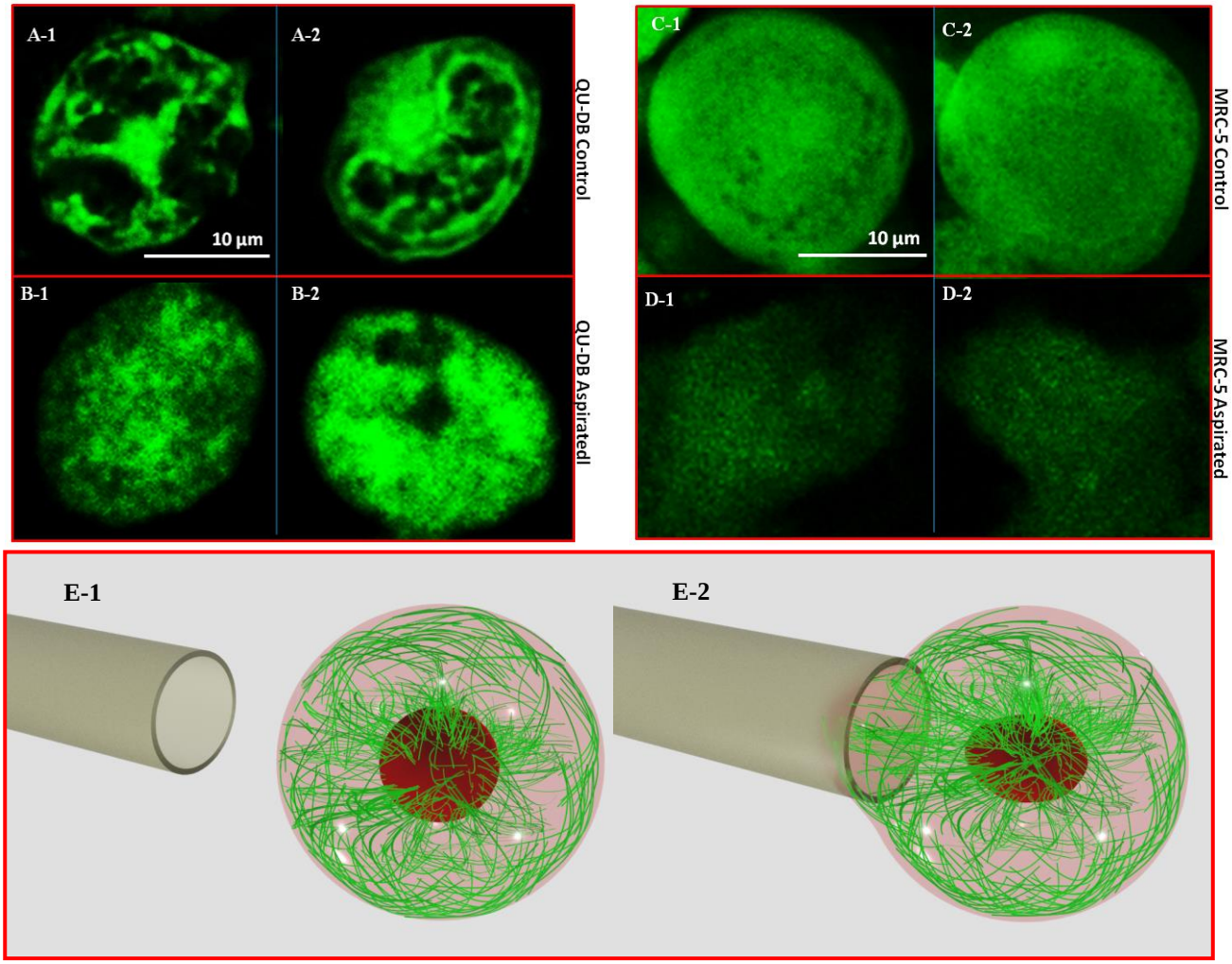

Figure 3. Confocal microscopy shows the effect of cancerous transformation and mechanical aspiration on remodelling (bundling) and alterations in actin microfilaments, respectively. Confocal microscopy images from non-aspirated QU-DB (A-1 and A-2) and MRC-5 (C-1 and C-2) cells together with aspirated cells of the same type (B-1, B-2 for QU-DB and D-1, D-2 for MRC-5). The illustrated images show that

the effect of the mechanical aspiration results in major alterations in the actin microfilaments. In addition, cancerous transformation resulted in the bundling of actin microfilaments. The schematic of E-1 and E-2 shows the actin microfilament distribution for non-aspirated and aspirated cells, respectively, in which the green lines represent actin microfilaments.

3.4 Role of actin microfilaments in the electromechanosensing of cancer cells.

It is worth noting that such behaviour is consistent with our quantitative model, given the expected dependence of electrical properties of aspirated healthy cells on alterations to the F-actin microfilament network. Actin filaments provide the essential infrastructure for sustaining cell morphology and functions and also regulate many fundamental cellular processes.[30] As shown in Figure 3 (Figure 3A vs. 3B, 3C vs. 3D and schematic 3E1 vs. 3E2), the cell aspiration process may result in major alterations in actin microfilaments.[31] Based on previous reports, the mechanics of the cytoskeleton may guide the response of diverse cells to the mechanical stress.[32,33] In this context, localised control of mechanical properties may enable us to engineer novel biomimetic approaches toward reconstituting further strong cell-like behaviours. However, actin microfilaments can modulate ion channel activity in the cell membrane as one of the fundamental bioelectronic elements of the cell.[34-37] Therefore, a strong correlation exists between the mechanical and electrical responses of aspirated normal cells based on actin activity. Furthermore, it was shown that microfilament disruption and remodelling would occur in malignant transformed cells.[38] In our investigation, comparative confocal microscopy images (Figures 3A vs. 3C and 4A vs. 4B) showed the distinct differences in actin microfilament configurations between the control samples of healthy and malignant lung cells. The images

show that the actin microfilaments are bundled and remodelled in QU-DB cells. Another indication of actin remodelling in malignant cells is shown in Figure 4.

Interestingly, the colour of the nucleus in the healthy (MRC-5) cell is orange and blurred (Figure 4-A), whereas this colour is clearly red for the stained malignant (QU-DB) cell (Figure 4-B). Because the observed colour for the stained nucleus is a reflection of the scanned laser from the samples, one can expect that the distribution of the actin microfilaments would strongly affect the reflection of the laser in healthy cells. However, no reflection of the laser from the stained nucleus was observed in cancer cells due to the disruption of actin. From these results, we propose that the actin microfilaments of a cancer cell may lose their function and natural resistance to mechanical stretching, which may not affect the ion channel activity in the membrane. Consequently, the influence of mechanical aspiration on the electrical impedance of a malignant cell may be disrupted. This model is consistent with disruptions that occur in the ion channel activity of cancerous transformed cells reported elsewhere.[3,39] A three-dimensional diagram from the electromechanical behaviour of MRC-5, QU-DB, HT-29 and SW-48 single cells is shown in Figure 4-C. The healthy cells clearly showed greater impedance changes from shorter stretched lengths, whereas cancerous progression resulted in lower impedance changes from longer stretched lengths using similar suction forces.

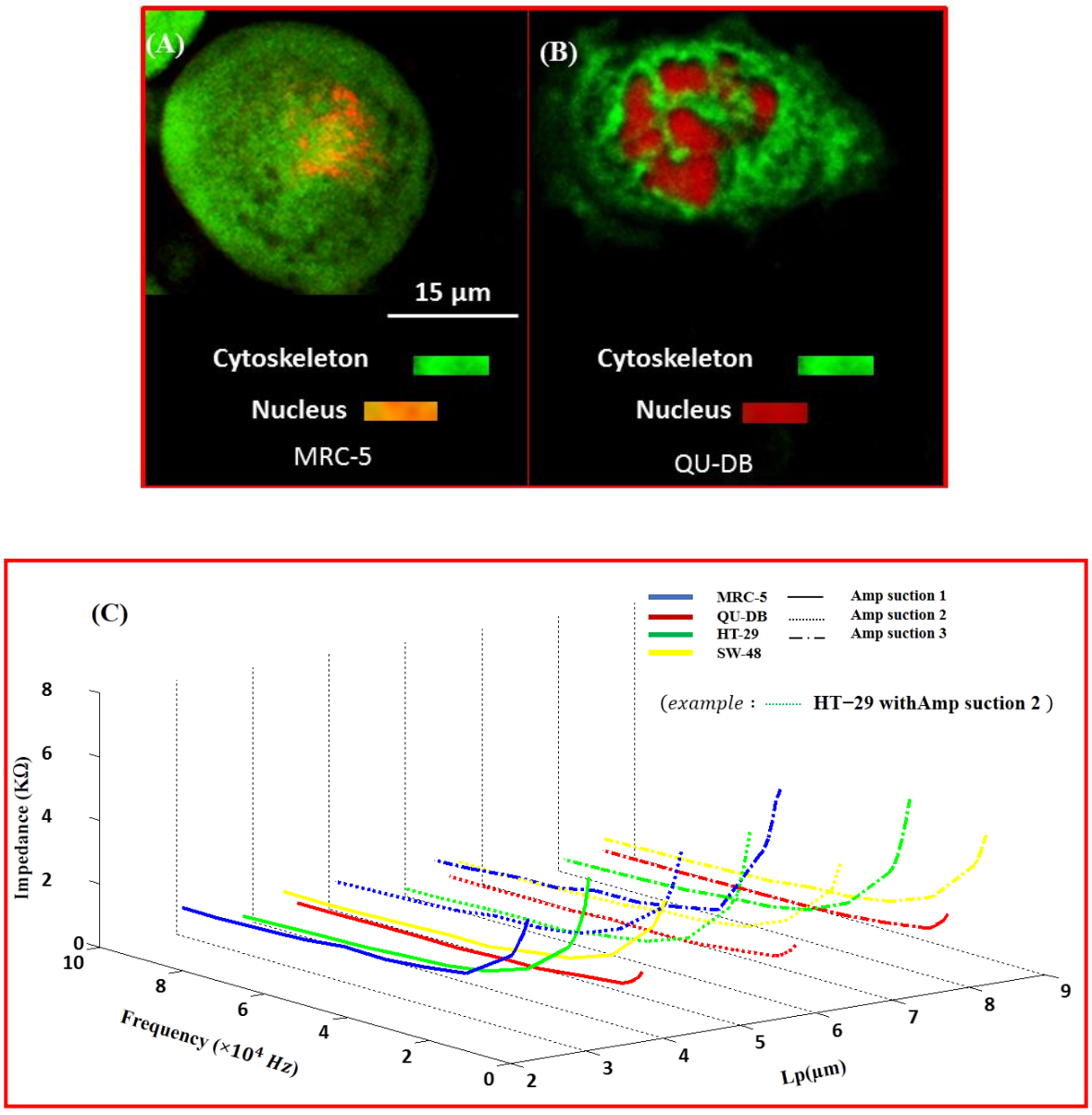

Figure 4. Differences in the electromechanical properties and F-actin distribution between normal and malignant cells are highly correlated. Comparative confocal microscopy images of control samples for A) healthy (MRC-5) and B) malignant (QU-DB) lung cells with PI-stained nuclei. C) 3D diagram of the variations in the electrical impedance of MRC-5, QU-DB, HT-29 and SW-48 single cells vs. frequencies ranging from 0.1 to 100 kHz due to the various lengths of the cell that flowed into the micropipette (Lp) via aspiration using three different suction amplitudes.

3.5 Electrical responses caused by cell retraction.

The impedance of aspirated MRC-5 cells was decreased following a minor retraction (Figure5 A-1 and A-2). The impedance measurement from a retracted cell may indicate the resilient effect of minor mechanical aspiration that can be observed in the bioelectronic parameters of the cell. In addition, a comparative investigation between the impedance of healthy and cancer cells aspirated by similar suction forces showed that the impedance (Figures 5 B-1 to B-3) and phase (Figure 5 B-4) of malignant cells are lower than those of healthy cells. These results are due to the lower sterol and phospholipid levels in malignant cells compared with normal cells.[40] Moreover, less rigidity (lower polarisation and limiting anisotropy) in the plasma membrane together with more unsaturation and fluidity of the phospholipids were observed in malignant cells.[41,42] Thus, the behaviour of highly mobile lipid bilayer cell membrane that electrically acts as an insulator or a dielectric layer[43] would be degraded by cancerous transformation. This would result in the lower impedance of cancer cells. Our results are consistent with other reports on the dielectric properties of healthy and malignant cells.[3,44]

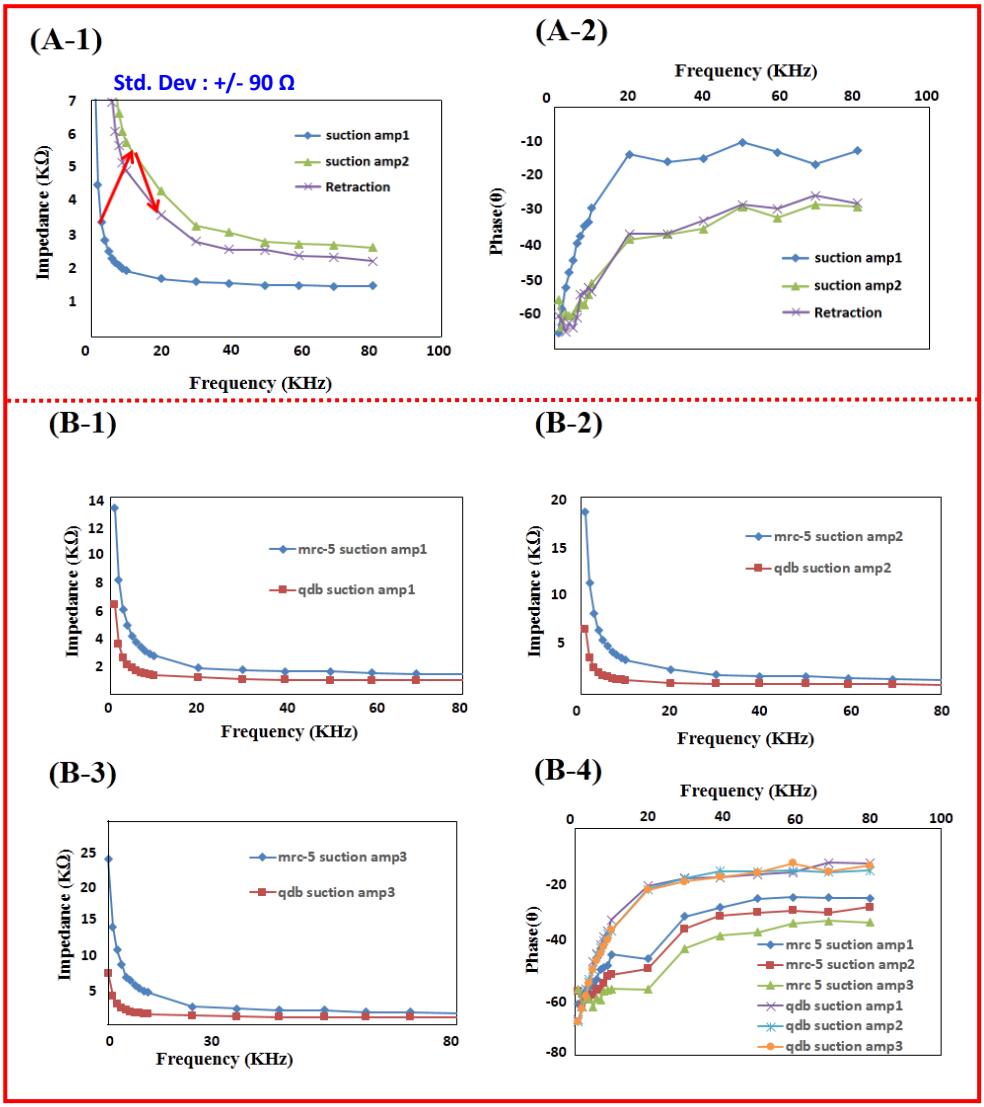

Figure 5. Minor mechanical retraction has a resilient effect on the electrical response of an aspirated cell. Effect of mechanical retraction on electrical impedance (A-1) and phase (A-2) of an aspirated MRC-5 cell. B) Comparative investigation between the impedance (B-1 to B-3) and phase (B-4) responses of aspirated healthy and cancer cells using the same range of suction forces.

These data demonstrate the capability of our correlative nanoelectromechanosensing system to introduce a new cancer diagnosis pattern by real-time recording of the electrical signals from mechanically stimulated cells using an 80-nm scale SiNT probe. Because the actin

microfilaments (as essential mechanical elements of cellular structure) play a key role in modulation of membrane ion channels (as critical subcellular organelles affect cellular bioelectrical behaviour), this system represents a clear and crucial application for cancer diagnosis for both research and clinical uses. Moreover, potential future applications, such as the effect of drugs on the mechanical and electrical properties of healthy and malignant cells (e.g., an extreme drug resistance assay) or the electromechanical stimulation and monitoring of stem cells in osteogenesis, could be monitored using this device.

4. Conclusion

In summary, the correlation between the mechanical rigidity and the electrical properties of a cell due to its cancerous state was monitored using a single-cell correlative electromechanosensing system in real-time as a new tool for cancer diagnosis. The general applicability of this approach was examined using lung and colon cell lines. Significantly, measuring the electrical response of a cell using a SiNT probe during aspiration with an electrically activated micropipette shows (i) a pronounced impedance increase when the healthy cell was stretched into the micropipette, and (ii) no observable impedance increase when the malignant cell was aspirated into the micropipette using the same suction forces. Confocal microscopy showed the crucial role of actin microfilaments in cells that had highly reduced electromechanical behaviour after metastatic progression. Our results demonstrate that such system can be used as a powerful nanobioelectromechanical tool for a new generation of label-free cancer diagnostics (could be applied for the unknown cancerous state cells extracted by biopsy, fine needle aspiration (FNA)

and pap smear) as well as for research in the field of single-cell bioengineering, having the ability to improve the monitoring and treatment of diseases.

Reference:

1 B. Szachowicz-Petelska, S. Sulkowski, and Z. A. Figaszewski, *Mol. Cell. Biochem.*, 2007, **294,** 237.

2 C. J. Field and P. D. Schley, *Am. J. Clin. Nutr.*, 2004, **79,** 1190S.

3 M. Abdolahad, M. Janmaleki, M. Taghinejad, H. Taghnejad, F. Salehia and S. Mohajerzadeh, *Nanoscale*, 2013, **5,** 3421.

4 M. Abdolahad, M. Taghinejad, H. Taghinejad, M. Janmaleki and S. Mohajerzadeh, *Lab Chip*, 2012, **12,** 1183.

5 E. Jonieztz, *Nature*, 2012, **491,** S56.

6 M. L. Yager, J. A. I. Hughes, F. J. Lovicu, P. W. Gunning, R. P. Weinberger and G. M. O'Neill, *Br. J. Cancer*, 2003, **89,** 860.

7 C. Lamaze, L. M. Fujimoto, H. L. Yin and S. L. Schmid, *J. Biol. Chem.*, 1997, **272,** 20332.

8 J. Pokorný, *J. Phys. Conf. Ser.*, 2011, **329,** 012007.

9 J. Pokorný, C. Vedruccio, M. Cifra and O. Kučera. *Eur. Biophys. J.*, 2011, **40,** 747.

10 J. Frede, S. P. Fraser, G. Oskay-Özcelik, Y. Hong, E. Ioana Braicu, J. Sehouli, H. Gabra, M. B. Djamgoz, *Eur. J. Cancer*, 2013, **49,** 2331.

11 Q. Qing, Z. Jiang, L. Xu, R. Gao, L. Mai and C. M. Lieber, *Nat. Nanotechnol.*, 2014, **9,** 142.

12 X. Duan, , T. M. Fu, J. Liu and C. M. Lieber, *Nano Today*, 2013, **8,** 351.

13 T. Luo, K. Mohan, P. A. Iglesias, and D. N. Robinson, *Nat. Mater.*, 2013, **12,** 1064.

14 Y. LeChasseur, S. Dufour, G. Lavertu, C. Bories, M. Deschênes, R. Vallée and Y. De Koninck, *Nat. Methods*, 2011, **8,** 319.

15 J. Dunlop, M. Bowlby, R. Peri, D. Vasilyev and R. Arias, *Nat. Rev. Drug Discov.*, 2008, **7,** 358.

16 A. Cohen, J. Shappir, S. Yitzchaik, and M. E. Spira, *Biosens. Bioelectron.*, 2006, **22,** 656.

17 M. Scanziani and M. Häusser, *Nature*, 2009, **461,** 930.

18 J. T. Davie, M. H. P. Kole, J. J. Letzkus, E. A. Rancz, N. Spruston, G. J. Stuart and M. Häusser, *Nat. Protoc.*, 2006, **1,** 1235.

19 A. Molleman, *Patch Clamping: An Introductory Guide to Patch Clamp Electrophysiology*. *John Wiley & Sons* 2003.

20 D. J. Banks, W. Balachandran, P. R. Richards and D. Ewins, *Physiol. Meas*, **23,** 437.

21 H. Taghinejad, M. Taghinejad, M. Abdolahad, A. Saeidi and S. Mohajerzadeh, *Sensors Actuators, B Chem.*, 2013, **176,** 413.

22 L. Xu, Z. Jiang, Q. Qing, L. Mai, Q. Zhang and C. M. Lieber, *Nano Lett.*, 2013, **13,** 746.

23 J. Yao, H. Yan, and C. M. Lieber, *Nat. Nanotechnol.*, 2013, **8,** 329.

24 G. Zheng, X. P. A. Gao and C. M. Lieber, *Nano Lett.*, 2010, **10,** 3179.

25 R. Gao, S. Strehle, B. Tian, T. Cohen-Karni, P. Xie, X. Duan, Q. Qing and C. M. Lieber, *Nano Lett.*, 2012, **12,** 3329.

26 J. Erickson, A. Tooker, Y. C. Tai and J. Pine, *J. Neurosci. Methods*, 2008, **175,** 1.

27 M. Reppel, F. Pillekamp, Z. J. Lu, M. Halbach, K. Brockmeier, B. K. Fleischmann and J. Hescheler, *J. Electrocardiol.*, 2004, **37,** 104.

28 TM. Fu, X. Duana, Z. Jiang, X. Dai, P. Xie, Z. Cheng and C. M. Lieber, *Proc. Natl. Acad. Sci. U. S. A.*, 2014, **111,** 1259.

29 H. Taghinejad, M. Taghinejad, M. Abdolahad and S. Mohajerzadeh, *Nanolett.*, 2013, **13**, 889**.**

30 R. D. Mullins, and S. D. Hansen, *Curr. Opin. Cell Biol.*, 2013, **25,** 1.

31 J. L. Drury, and M. Dembo, *Biophys. J.*, 2001, **81,** 3166.

32 M. Aragona, T. Panciera, A. Manfrin, S. Giulitti, F. Michielin, N. Elvassore, S. Dupont and S. Piccolo, *Cell*, 2013, **154,** 1047.

33 M. Fritzsche, A. Lewalle, T. Duke, K. Kruse, and G. Charras, *Mol. Biol. Cell*, 2013, **24,** 757.

34 S. C. Calaghan, J. Y. Le Guennec and E. White, *Prog. Biophys. Mol. Biol.*, 2004, **84,** 29.

35 H. F. Cantiello, *Kidney Int.*, 1995, **48,** 970.

36 W. X. Xu, S. J. Kim, I. So, and K. W. Kim, *Pflugers Arch. Eur. J. Physiol*, 1997**, 434,** 502.

37 X. Yang, P. J. I. Salas, T. V. Pham, B. J. Wasserlauf, M. J. D. Smets, R. J. Myerburg, H. Gelband, B. F. Hoffman and A. L. Bassett, *J. Physiol.*, 2002, **541,** 411.

38 B. Lomenick, R. Hao, N. Jonai, R. M. Chin, M. Aghajan, S. Warburton, J. Wang, R. P. Wu, F. Gomez, J. A. Loo, J. A. Wohlschlegel, T. M. Vondriska, J. Pelletier, H. R. Herschman, J. Clardy, C. F. Clarke and J. Huang, *Proc. Natl. Acad. Sci. U. S. A.*, 2009, **106,** 21984.

39 K. Kunzelmann, *J. Membr. Biol.*, 2005, **205,** 159.

40 H. R. Byers, T. Etoh, J. R. Doherty, A. J. Sober, and M. C. Mihm, *Am. J. Pathol.*, 1991, **139,** 423.

41 A. B. Kier and C. Franklin, *Invasion Metastasis*, 1991, **11,** 25.

42 N. Sperelakis , Cell Physiology Source Book, 4th Edition *Elsevier*, 2011

43 P. A. Janmey and P. K. J. Kinnunen, *Trends Cell Biol.*, 2006, **16,** 538.

44 M. Abdolahad, H. Shashaani, M. Janmaleki, and S. Mohajerzadeh, *Biosens. Bioelectron.*, 2014, **59,** 151.